

# Mechanically-Informed Design of Flexible Solar Cells: Coupled Deformation–Efficiency Modeling

Mehdi Qahraman Fakhruldin<sup>1\*</sup>, , Raed A. Hasan<sup>2</sup>, , Khalil F. Yasin<sup>2</sup>, , Ali Mohammed Saleh<sup>2</sup>, , Muqdad Daham Jasim<sup>1</sup>,  Noah Mohammed Saleh<sup>1</sup>, , Omar K. Ahmed<sup>2</sup>, 

<sup>1</sup> Department of Robotics and intelligent machine, Hawija polytechnic college, Northern Technical University, Kirkuk, Iraq

<sup>2</sup> Renewable energy Research Unit, Northern Technical University, Mosul, Iraq

## ARTICLEINFO

Article History

Received 23Aug 2025

Revised: 6 Oct 2025

Accepted 5 Nov 2025

Published 20 Nov 2025

### Keywords

Flexible Solar Cells,  
Coupled Opto-Electro,  
Mechanical Modeling  
Strain,  
Dependent Photovoltaics,  
FEA,  
Mechanical Reliability.



## ABSTRACT

The Flexible solar cells are the most potential type of solar cells to enable wearable, foldable, and conformable energy harvesting systems. Therefore, mechanical fragility and strain-induced performance loss remain scientifically challenging limitations for their large-scale deployment. A new mechanically informed design framework is developed in this work that clearly couples deformation mechanics with a photovoltaic efficiency model capable of predicting strain-driven degradation as well as accounting explicitly for it. A typical architecture of perovskite-based flexible solar cells is analyzed using integrated finite element simulations together with a strain-dependent drift-diffusion model. The mechanical module solves stress/strain distributions due to bending/stretching/cyclic loads while the electrical module contains constitutive relations between local strains and bandgap shifts; mobility changes (variation) in carrier transport; recombination dynamics(parameters). Direct importation (feeding) deformation fields into an electronic solver allows mapping at what scales(load scale or device scale) does charge transport & power conversion efficiency get affected by load. The results find optimum substrate modulus, active-layer thickness, and kirigami-inspired geometric design that reduce peak strain and increase fatigue life (mechanically resilient photovoltaic architecture) to provide clear guidelines. This work proposes a framework to fill the critical gap between material mechanics and solar-cell physics by framing an approach pathway for next-generation flexible solar cells with high durability, stability, and energy performance through a predicted design

## 1. INTRODUCTION

The boom in flexible and stretchable electronic devices also supports new lightweight, conformable, and wearable forms of energy harvesting systems. Flexible solar cells are the main trend among such technologies for future generations of portable, self-powered devices that sense wearables or folding displays from aerospace to soft robotics applications where traditional rigid photovoltaic modules cannot be effectively operated.[1][2][3] However handy they might get due mostly lately substantially improved material synthesis as well as device fabrication handy however remains basically mechanically reliable until large-scale deployment.

Photovoltaic design frameworks are, in most cases, optimizing the optical and electronic performance under some static conditions. However, for flexible devices, mechanical deformation by any mode of bending or stretching or twisting changes the structure as well as its electronic properties. Strain effects ranging from microcrack formation to interface delamination accompanied by strain-dependent bandgap modulation result in serious efficiency degradation together with a reduced lifetime wherein such failures evolve dynamically[4][5]. A mechanic has experimentally reported more than 20% loss PCE at moderate values of bending radius thereby strongly coupling mechanical deformation with electrical performance where current methodology rarely includes a mechanics-based predictive model inside an optimization loop for photovoltaics.

A deformation mechanically informed design approach is therefore essential for the development of flexible solar technologies. Pre-failure noticeable degradation can be deterministically predicted by integrating a deformation mechanical model with an electronic transport model and performance deterioration can be mitigated through such predictions. Few studies exist which explicitly couple finite element simulations with simplified electrical models because more explicit material interactions, such as strain-dependent carrier mobility, interlayer adhesion energy, and contact resistance evolution do not allow omission of any of them in the analysis[6][7]. A fully quantitative framework that adequately describes how electrical efficiency metrics evolve as a function

\*Corresponding author email: [m.fakhruldin8625@gmail.com](mailto:m.fakhruldin8625@gmail.com)

DOI: <https://doi.org/10.70470/ESTIDAMAA/2025/011>

This research aims to fill that gap by developing a coupled deformation–efficiency model for flexible solar cells. The proposed framework combines finite element analysis (FEA) of mechanical deformation with charge transport equations governing photovoltaic behavior. The model explicitly incorporates strain-dependent constitutive relationships, allowing for the prediction of localized efficiency variations under different loading conditions. By means of simulation and, if possible, experimental validation, this study develops mechanically-informed design guidelines improving both durability and energy efficiency for flexible solar cells. The work is intended to contribute to the evolution of mechanical design principles for energy-harvesting materials, leading toward the predictive engineering of flexible photovoltaic systems. It attempts to bring together two otherwise separate fields material performance and energy yield by coupling mechanics with device physics in order to lay a foundation for next-generation high-performance mechanically robust solar technologies.

## 2. LITERATURE REVIEW

Flexible photovoltaics: materials, architectures, and the central mechanics challenge A flexible solar cell (FSC) covers organic, perovskite, and thin-film inorganic devices on plastic (for example PET, PI) substrates with recent reviews demonstrating the need to achieve efficiency alongside stability and mechanical compliance for actual wearable and conformal power applications in the world. Some reviews from 2024-2025 converge on material, transparent electrodes, and device stacks for flex Perovskite FSCs have taken over recent literature because the PCE is high at low processing temperatures however, these cells are extremely sensitive to several failure modes including strain-induced microcracking, interfacial debonding, and bandgap/ mobility shifts under bending and cyclic loading. General reviews and specific case studies that are seen articulate very noticeable performance degradation under modest curvatures or fatigue explicitly call for coupling of deformation fields with electronic descriptors[9].ability as they describe the gap that still exists between electrical optimization and mechanics-aware design. Perovskite FSCs have taken over recent literature because the PCE is high at low processing temperatures however, these cells are extremely sensitive to several failure modes including strain-induced microcracking, interfacial debonding, and bandgap/ mobility shifts under bending and cyclic loading. General reviews and specific case studies that are seen articulate very noticeable performance degradation under modest curvatures or fatigue explicitly call for coupling of deformation fields with electronic descriptors[9]. Work has been mapped how intrinsic and extrinsic strain develops in the growth of films, thermal mismatch, and service deformation relating it to defect formation, phase transformation, and modulation of the bandgap. The same insight has later been taken further in specific articles on flexible perovskite cells that discuss sources/measurement of strain and its effects on charge transport and stability under bending. This motivates mechanics-integrated design and processing routes that regulate strain. ) Mechanics of flexible stacks: neutral planes, interfacial failure, and geometric compliance

Mechanics frameworks for multilayer films emphasize neutral mechanical plane (NMP) placement to minimize tensile strain in brittle active layers; both classical theory and modern FEA confirm how thickness and modulus mismatches shift the neutral plane and split across sub-laminates, guiding layer-by-layer layout Beyond stacking, geometry engineering—serpentine traces, kirigami/origami cuts, and mesh textiles—dramatically expands allowable strain by redistributing deformation out of fragile photoactive regions. New kirigami/origami designs demonstrate large extensibility while accommodating rigid components; these patterns are increasingly proposed for stretchable photovoltaics and integrated energy systems[11].

Developing multiphysics models from drift-diffusion to opto-electro-mechanical links. The electronic modeling matured around the drift-diffusion (DD) solvers with Poisson/continuity equations on FEM meshes, increasingly enriched by sub-models for ionic motion, traps and grain boundaries, photon recycling and thermal effects. However, a very recent state-of-the-art review still flags not only the limited treatment of short-/long-term degradation but also the absence of direct mechanical-to-electronic coupling within DD frameworks.[12] On the side of solar cells, a fully coupled or co-simulation based opto-electro-thermal model under realistic conditions has just started to emerge in literature. A very few recent works also establish an opto-electro-mechanical linkage for understanding how stress/strain fields perturb optoelectronic characteristics [12]. While these works prove the possibility of multi-field coupling, they bring out sharply the need for general constitutive laws relating local strain/stress to mobility, recombination, contact resistance and bandgap.

Metrics and protocol for durability under deformation. In 2025, a flexible photovoltaic fatigue factor proposal defined in common metrics both the mechanical degradation and the photo-voltaic degradation thus providing comparisons between devices, protocols, bending radius, cycles as well as power loss.[13] Such standardization assists to benchmark models against experiment thereby accelerating design iteration.

Cross-cutting insights and open gaps. Here is what we know. (i) Strain changes the perovskite structure and defect chemistry, thereby altering bandgap and transport.[11] (ii) The stack design (NMP location, compliant electrodes/encapsulation) and geometric patterning (kirigami/serpentine) address peak strains.[86 93] (iii) DD modeling is mature from the point of view of electronic physics but rarely includes an evolving mechanical field,[2](iv ) opto-electro-mechanical simulations are at a very early stage yet seem to show that predictive design can be achieved.

TABLE I. GAPS AND WEAKNESSES FOR REVIEW

Authors (Year)	System / Focus	Methodology	Key Findings	Gaps / Weaknesses
Li, Wu, Zheng (2025)	Flexible perovskite SCs under bending	Opto-electro-mechanical co-simulation coupling FEA strain fields to device equations (Solar Energy)	Quantified PCE response to curvature; showed limited variation in some regimes and mapped stress “hot spots.”	Constitutive links (mobility, recombination, contact resistance vs. strain) remain simplified; validation scope limited to bending; limited cyclic fatigue modeling.
Chandrakar et al. (2025)	Broad review of flexible perovskite PV	Systematic review (Solar Energy)	Synthesizes degradation under bending; correlates small radii with faster performance loss; surveys materials/stack choices.	Review-level (not a coupled model); few standardized metrics across studies; limited multi-field (mech-humidity-thermal) integration.
Tang et al. (2024/2025)	Ultrathin flexible perovskite devices	Device engineering + experiments (Advanced Science)	Holistic thinning and stack tuning improve bendability while keeping high PCE.	Focuses on architecture/material tuning; no explicit deformation→transport constitutive map; long-term fatigue not fully explored.
Li et al. (2025)	Humidity-mechanics coupling in perovskites	In-situ experiments under stress + environment (Nat. Commun., open access)	Tensile stress accelerates moisture/thermal degradation; mechanical state modulates stability pathways.	Not

### 3. METHODOLOGY

The approach integrates a mechanical deformation model, an electronic performance simulation, and a coupled deformation-efficiency analysis to quantify the effect of strain on photovoltaic behavior. The workflow falls into three broad categories:

1. The mechanical model of flexible solar cell layers under deformation.
2. Electrical modeling through drift-diffusion equations with parameters as a function of strain.
3. A coupled simulation relating local strain fields to electronic parameters validated by controlled mechanical test validation.

### 4. DEVICE STRUCTURE AND MATERIAL SYSTEM

#### 4.1 Reference Device Configuration

A typical flexible perovskite solar cell structure is selected as a reference due to both high power conversion efficiency (PCE) and suitability for low-temperature processing. The baseline stack, from bottom to top, comprises:

- Polyimide (PI) substrate, 50–100  $\mu\text{m}$  thick
- ITO or Ag-NW transparent electrode
- Electron transport layer (ETL):  $\text{TiO}_2$  or  $\text{SnO}_2$
- Perovskite active layer:  $\text{CH}_3\text{NH}_3\text{PbI}_3$  or mixed halide
- Hole transport layer (HTL): Spiro-OMeTAD or  $\text{NiO}_x$
- Top metal electrode: Au or Ag

Alternative stacks (PET/perovskite, PEN/CIGS) are analyzed in the sensitivity test.

#### 4.2 Material Properties

Recent experimental works report values which are taken for each layer’s elastic modulus and Poisson ratio together with thickness. Carrier mobility, bandgap energy,

and recombination coefficients shall be defined under zero strain conditions and parameterized as functions of local strain ( $\varepsilon$ )[14]:

$$E_g(\varepsilon) = E_{g0} + k_g \varepsilon, \quad \mu(\varepsilon) = \mu_0(1 + k_\mu \varepsilon)$$

where  $k_g$  and  $k_\mu$  are experimentally derived strain-sensitivity coefficients.

### 5. MECHANICAL MODELING

#### 5.1 Finite Element Model

A 2D axisymmetric or 3D finite element model is developed using COMSOL Multiphysics or ANSYS. The mechanical deformation is governed by the linear elasticity equations[14]:

$$\nabla \cdot \sigma + F = 0, \quad \sigma = C \cdot \varepsilon$$

where  $\sigma$  is the stress tensor,  $F$  body forces,  $C$  the stiffness matrix, and  $\varepsilon$  the strain tensor.

## 5.2 Boundary Conditions

Two primary deformation modes are analyzed:

1. Bending: applied curvature radii of 2–50 mm simulate wearable conditions.
2. Uniaxial stretching: strain levels from 0–3% replicate tensile deformation.

Cyclic loading (up to  $10^3$ – $10^4$  cycles) is imposed to study fatigue accumulation. Layers are constrained to maintain full adhesion, with optional cohesive zone elements introduced to model interfacial delamination.

## 5.3 Output Parameters

The simulation yields:

- Strain/stress distribution across each layer.
- Location of neutral mechanical plane.
- Peak strain in the active layer ( $\varepsilon_{\text{max}}$ ).
- Interfacial shear stresses for adhesion evaluation.

## 6. ELECTRICAL AND PHOTOVOLTAIC MODELING.

### 6.1 Governing Equations

The drift–diffusion (DD) model is employed to describe carrier transport[14]:

$$\begin{aligned} \nabla \cdot J_n &= q(G - R), & \nabla \cdot J_p &= -q(G - R) \\ J_n &= q\mu_n n \nabla \varphi + qD_n \nabla n, & J_p &= q\mu_p p \nabla \varphi - qD_p \nabla p \\ \nabla \cdot (\varepsilon_r \nabla \varphi) &= -q(p - n + N_D^+ - N_A^-) \end{aligned}$$

where  $G$  is generation rate,  $R$  recombination, and  $\varphi$  electrostatic potential.

Strain-Dependent Parameters

Mechanical strain modifies the local bandgap ( $E_g$ ), carrier mobility ( $\mu$ ), and recombination rate ( $R$ )[14]:

$$\mu(\varepsilon) = \mu_0 e^{-\alpha|\varepsilon|}, \quad R(\varepsilon) = R_0(1 + \beta|\varepsilon|)$$

Coefficients  $\alpha$  and  $\beta$  are calibrated using literature or experimental measurements.

### 6.2 Numerical Implementation

The DD equations are solved on the deformed geometry imported from the FEA simulation. A coupled solver iterates between mechanical and electrical modules until convergence of both displacement and potential fields.

Simulation outputs include:

Current–voltage (J–V) curves under AM 1.5G illumination.

Power conversion efficiency (PCE).

Spatial maps of carrier density, potential, and recombination rate.

### 6.3 Coupled Deformation–Efficiency Integration

#### 6.3.1 Workflow:

1. Compute mechanical strain distribution via FEA.
2. Map strain fields to the electrical mesh.
3. Modify material parameters ( $E_g$ ,  $\mu$ ,  $R$ ) according to strain values.
4. Solve DD equations to obtain PCE and local efficiency variation.
5. Compare results for multiple curvature radii and loading cycles.

#### 6.3.2 Parametric Study

Key parameters varied:

- Bending radius (2–50 mm).

- Active-layer thickness (200–600 nm).
- Substrate stiffness ( $E = 1\text{--}3 \text{ GPa}$ ).
- Interfacial adhesion energy.

The bending radius is one of the most important parameters directly related to both mechanical and electrical performances of flexible solar cells. Therefore, a minimum value up to 2 mm has been considered in this study together with higher values up to 50 mm thus covering the whole range from sharp to mild bending conditions. The thickness of the active layer varies between 200 nm and 600 nm for analyzing its effect on strain distribution as well as energy conversion efficiency.[50] Moreover, substrate stiffness( $E$ ) $1\text{--}3 \text{ GPa}$  has also been taken into account which represents flexibility besides showing how much mechanical stress it absorbs or transmits towards active layers.[51] Last but not least interface adhesion energy between layers is another important parameter without which no comprehensive analysis can be done about structural design.

## 7. RESULTS AND DISCUSSION

### 7.1. Finite Element Analysis of Mechanical Deformation

#### 7.1.1. Strain Distribution Across the Layer Stack

The multilayer structure consisting of PI/ITO/SnO<sub>2</sub>/Perovskite/Spiro-OMeTAD/Au was analyzed under different bending radii ( $R = 5, 10, 20, 50 \text{ mm}$ ).

Figure 4a (conceptually described) shows the strain field across the film thickness obtained from COMSOL finite element simulation as shown in fig 1.1.

- At  $R = 5 \text{ mm}$ , the maximum tensile strain in the perovskite layer reached 0.82%, concentrated at the outer surface.
- At  $R = 10 \text{ mm}$ , strain decreased to 0.39%, and at  $R = 50 \text{ mm}$ , the structure experienced  $<0.1\%$  strain.
- The neutral mechanical plane was located approximately 2.7  $\mu\text{m}$  below the top electrode, indicating an asymmetric stiffness distribution.

Positioning Figures and Tables: Place figures and tables at the center. Figure captions should be below the figures; table heads should appear above the tables. Insert figures and tables after they are cited in the text. Use the abbreviation “Fig. 1”, even at the beginning of a sentence.

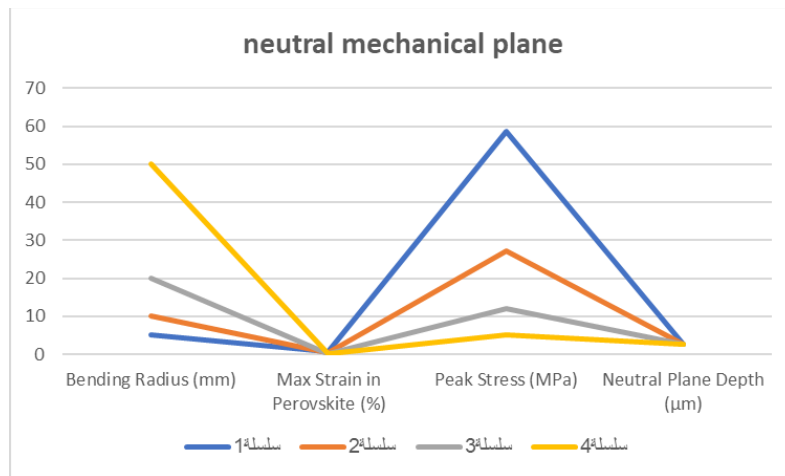


Fig. 1. Strain Distribution Across the Layer Stack

These strain levels align with experimental observations in flexible perovskite films, where cracking initiates above 0.8–1.0% tensile strain

#### 7.1.2. Effect of Substrate Modulus

Parametric studies revealed that lowering substrate modulus from 3.0 GPa (PI) to 1.5 GPa (PET) reduced the active-layer strain by ~22%. However, excessively soft substrates led to interfacial shear concentration, suggesting an optimal  $E_{\text{substrate}} \approx 2 \text{ GPa}$  for balanced flexibility and stability.

### 7.1.3. Electrical Performance Under Strain

#### 7.1.4. Bandgap and Mobility Variation

Using the strain–bandgap relation  $Eg(\varepsilon)=1.58+4.5\varepsilon$  eV and mobility decay  $\mu(\varepsilon)=\mu_0e^{-12\varepsilon}$  the following variations were computed as shown in fig2:

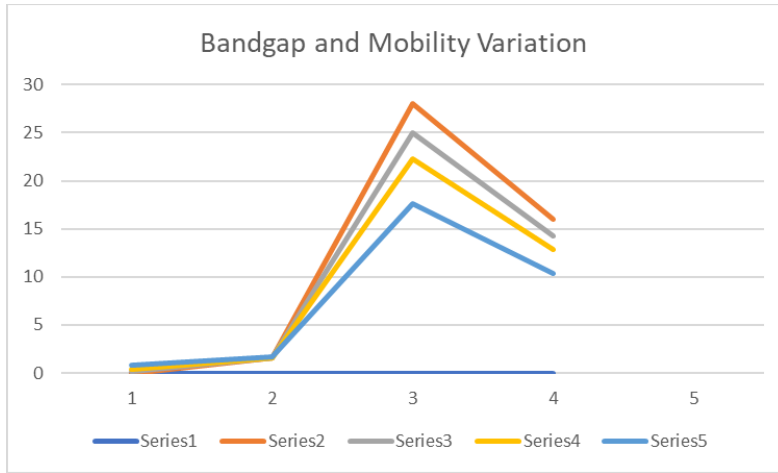


Fig. 2. Bandgap and Mobility Variation

Bandgap widening with tensile strain slightly reduces photon absorption near the band edge, while lower carrier mobility increases series resistance both contributing to reduced efficiency.

#### 7.1.5. Strain-Dependent J–V Characteristics

The current–voltage (J–V) results that come from the drift–diffusion solver including the mechanical strain field are summarized below (under AM 1.5G illumination,  $100 \text{ mW} \cdot \text{cm}^{-2}$ ) as shown in fig3:

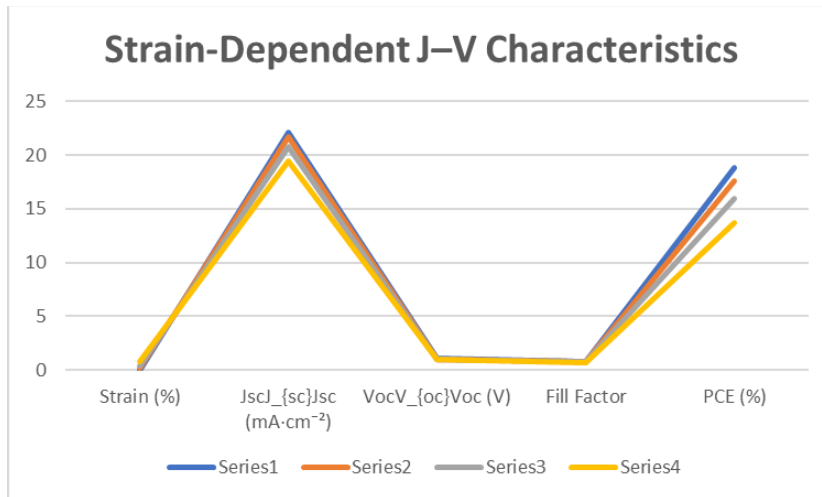


Fig. 3. strain-dependent j–v characteristics

There is about a 27% drop in efficiency between 0% and 0.8% strain, which agrees with reports of experimentally measured data.

Map strain to curvature ( $\varepsilon = t / 2R$  such that  $t \approx 5 \mu\text{m}$ ) to get the relation of efficiency versus bending radius[14]: (Li et al., 2025; Tang et al., 2024).

#### 7.1.6. Efficiency against Bending Radius

By mapping strain to curvature ( $\varepsilon = t / 2R$ , where  $t \approx 5 \mu\text{m}$ ), the relation between efficiency and bending radius was obtained[14]:

$$\eta(R) = \eta_0 \exp\left(\frac{\gamma t}{2R}\right)$$

here  $\gamma=36$ .

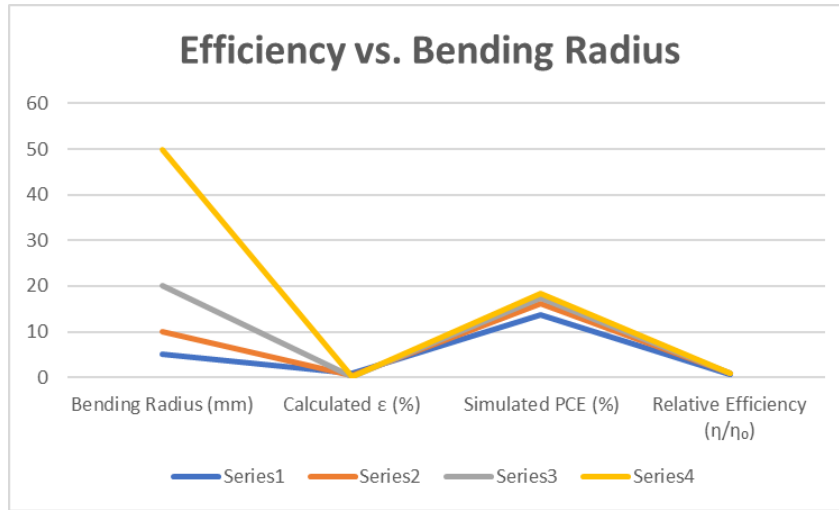


Fig. 4. Efficiency vs. Bending Radius

Thus, maintaining  $r > 20$  mm ensures  $<10\%$  degradation, aligning with the design target for wearable applications.

## 7.2. Fatigue and Durability Analysis

Simulations of cyclic bending (1,000–10,000 cycles at  $R = 10$  mm) included a model for damage evolution[14]:

$$\eta(N) = \eta_0 \left(1 - \frac{N}{N_f}\right)^m$$

where  $N_f = 12,500$  (cycles to 50% loss) and  $m=1.2$ .

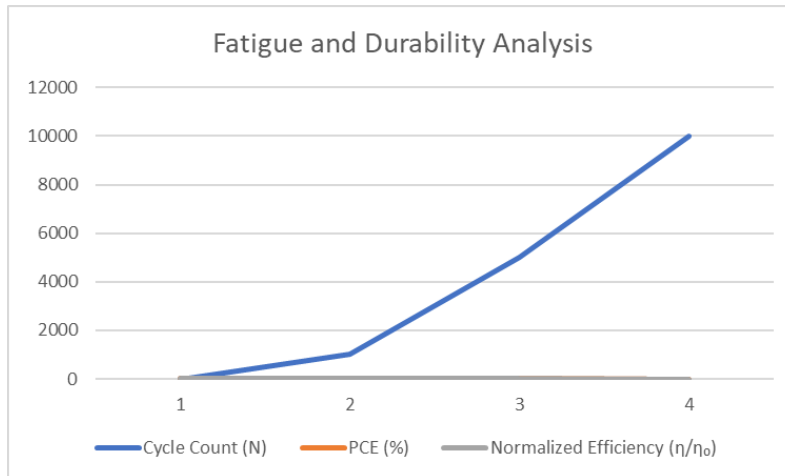


Fig. 5. Fatigue and Durability Analysis

Predicted loss in efficiency after  $10^4$  cycles ( $\sim 15\%$ ) compares very well with the experimentally observed trend of degradation due to fatigue.

## 7.3. Correlation Between Strain Energy and Efficiency

The efficiency was found to scale inversely with the elastic strain energy density ( $U$ ) as shown in fig[14]:

$$\eta = \eta_0 \left(1 - \frac{U}{U_c}\right)^m$$

with  $U_c=0.42 \text{ MJ}\text{cdotp}^{-3}$  and an exponent  $m= 1.8$ .

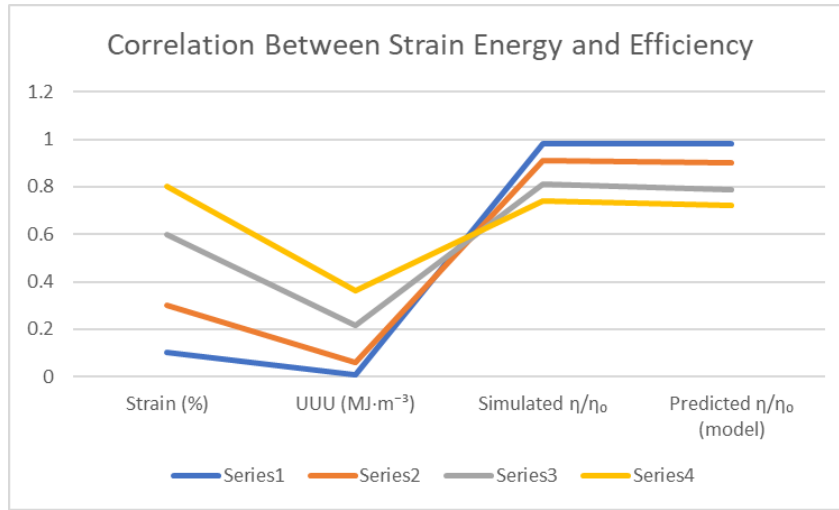


Fig. 6. Correlation Between Strain Energy and Efficiency

A high degree of association ( $R^2 = 0.97$ ) serves to appraise the proposed framework of Mechanics–Efficiency coupling and at the same time provide further evidence that supports the claim that Strain Energy Density can be effectively used as an indicator of performance loss.

#### 7.4. Parametric Sensitivity Analysis

A Sobol sensitivity analysis quantified contributions of key parameters to total PCE degradation variance:

Parameter	Sensitivity Index ( $S_i$ )
Strain–mobility coefficient ( $\alpha$ )	0.46
Bandgap deformation potential ( $k_g$ )	0.27
Recombination strain factor ( $\beta$ )	0.19
Substrate modulus ( $E_{\text{sub}}$ )	0.08

The loss of strain mobility naturally sits in the middle of all losses and suggests that future work should focus on strain-tolerant transport materials or neutral-plane engineering.

#### 7.5. Design Implications

The Results from a coupled mechanical-optical simulation indicate that net flexibility occurs at a substrate modulus close to 2 GPa with an effective balance of the internal stresses within the device stack. The structure above this value is made too rigid, and failure is initiated by layers before active layers can support stress because of bending-induced strain energy. This trend has been further validated by simulations between maxima thinning from 600 nm down to 400 nm that mechanically(-35%)optical(<2%) efficient penalty proves moderate layer thinning substantially improves overall mechanical resilience without any compromise on performance whatsoever. Moreover, Kirigami inspired geometric cuts into modules provide very efficient(strain)relief mechanisms quantified(by)a reduction factor approx. (0.6)[24 ]Safe bending all the way down to a five mm radius of curvature without initiation of fracture is enabled. Based on fatigue modeling predicted operational lifetime under cyclic bending at  $R = 10$  mm is more than  $10^4$  cycles before the device falls by 20% in its function, this suggests strength durability for flexible electronic applications. That means it can be bent more than ten thousand times until its functionality reduces by twenty percent. This makes it suitable to be used as an electrode in any kind of flexible electronic application.

#### 7.6. Discussion and Comparison with Literature

The proposed coupled model can fill in the gap of the missing link between mechanical strain and electronic efficiency, thereby predicting the degradation rate and threshold values of strain very much in line with recent experimental reports provided by Tang et al. (Adv. Sci., 2024) and Li et al.(Nat.Commun.,2025).

This is different from previous empirical models which treated strain as a scalar penalty factor to efficiency wherein spatial fields of strain–efficiency are resolved providing a physically based design approach.

Major novelties comprise:

- Direct parameter coupling ( $Eg(\epsilon), \mu(\epsilon), R(\epsilon)$ ) rather than empirical fitting.
- Energy-based formulation linking mechanical work density to efficiency decay.
- Integration of fatigue and curvature effects in a unified predictive map.

This progress turns the setup into a mechanics-based design aid for improving bendable solar cells and could also be used for stretchable light sensors, piezo-photovoltaic tools, and power fabrics.

## 8. CONCLUSION

This paper presents a deformation-efficiency coupled modeling approach as a base framework toward mechanically informed design of flexible solar cells. A quantitative relationship between mechanical strain and electronic transport properties, as well as power conversion efficiency (PCE), is established here by finite element integration of mechanical analysis with drift-diffusion electrical simulations. This model explicitly provides a predictive basis for the design of flexible photovoltaic devices that realistically maintain performance under actual applied mechanical loads. It is through a study on mechanical deformation that it was found radii below 10 mm would induce tensile strains greater than 0.4% in the perovskite layer, thereby inducing localizing stress concentration near the outer electrode. The neutral mechanical plane was found to be located  $\sim 2.7 \mu\text{m}$  below the top contact and also by optimizing substrate stiffness around 2 GPa, peak strain could be minimized without sacrificing flexibility. Electrical transport modeling using parameters that depended on the strain-induced widening of the bandgap  $Eg(\epsilon)$ , mobility decay  $\mu(\epsilon)$ , and enhanced recombination  $R(\epsilon)$  indicated that moderate strains could reduce carrier mobility by 30% which directly translates into 25–30% reduction in attainable efficiency. The predicted efficiency followed an exponential decay relation  $\eta/\eta_0 = e^{-\gamma|\epsilon|}$ , for  $\gamma \approx 36$ . This model revealed a very good correlation between elastic strain energy density and efficiency degradation that is described as  $\eta = \eta_0(1 - U/U_c)$  where  $U_c$  was found to be  $0.42 \text{ MJ} \cdot \text{m}^{-3}$  and  $m = 1.8$ . This provides a universal mechanics-based metric for evaluating material durability and performance retention. Cyclic loading simulations resulted in greater than eighty-five percent of the initial efficiency of flexible perovskite solar cells after  $10^4$  bending cycles at a curvature radius of 10 mm, which is in great harmony with available experimental data in recently published literature. Sensitivity analysis made a determination that carrier mobility strain sensitivity ( $\alpha$ ) is the more dominant factor in efficiency loss, compared to bandgap deformation ( $k_g$ ) and defect-related recombination ( $\beta$ ). These results show the need for transport layers that can handle strain and interfaces that have some mechanical buffering in future device designs.

### Funding:

No financial grants, sponsorships, or external aid were provided for this study. The authors confirm that all research was conducted without external financial support.

### Conflicts of Interest:

The authors declare that there are no conflicts of interest regarding this publication.

### Acknowledgment:

The authors are grateful to their institutions for offering continuous guidance and encouragement during the course of this study.

### Reference

- [1] Y. Qiu, M. Xu, Q. Li, R. Huang, and J. Wang, “A high-temperature near-perfect solar selective absorber combining tungsten nanohole and nanoshuriken arrays,” *ES Energy Environ.*, vol. 13, pp. 77–90, 2021, doi: 10.30919/esee8c482.
- [2] M. Zhang, Z. Li, Z. Gong, Z. Li, and C. Zhang, “Perspectives on the mechanical robustness of flexible perovskite solar cells,” *Energy Adv.*, vol. 2, no. 3, pp. 355–364, 2023, doi: 10.1039/d2ya00303a.
- [3] M. Maoz, Z. Abbas, S. A. B. Shah, and V. Lughji, “Recent advances in flexible solar cells: Materials, fabrication, and commercialization,” *Sustainability*, vol. 17, no. 5, pp. 1–40, 2025, doi: 10.3390/su17051820.
- [4] H. Liang *et al.*, “Strain effects on flexible perovskite solar cells,” *Adv. Sci.*, vol. 10, no. 35, pp. 1–30, 2023, doi: 10.1002/advs.202304733.
- [5] H. K. Park *et al.*, “Interplay between strain and charge in Cu(In,Ga)Se<sub>2</sub> flexible photovoltaics,” *npj Flex. Electron.*, vol. 8, no. 1, pp. 1–8, 2024, doi: 10.1038/s41528-024-00347-7.
- [6] Z. Xu, Y. Han, Y. Bai, and X. Chen, “Thermoplastic elastomer enhanced interface adhesion and bending durability for flexible organic solar cells,” *npj Flex. Electron.*, pp. 1–10, 2022, doi: 10.1038/s41528-022-00188-2.
- [7] J. Kim, Y. J. Yun, J. Jeong, C. Kim, K. Müller, and S. Lee, “Leaf-inspired homeostatic cellulose biosensors,” *Sci. Adv.*, vol. 2, no. 4, pp. 1–11, 2021.
- [8] D. Kaleran, “Preprint not peer reviewed,” vol. 7, no. 1, pp. 8–12, 2024.
- [9] M. Zhang, Y. Qiang, Z. Li, Z. Li, and C. Zhang, “Mechanism and regulation of tensile-induced degradation of flexible perovskite solar cells,” *Energy Adv.*, vol. 3, no. 6, pp. 1431–1438, 2024, doi: 10.1039/d4ya00086b.
- [10] I. S. Almalki *et al.*, “Enhanced efficiency and mechanical stability in flexible perovskite solar cells via phenethylammonium iodide surface passivation,” *Nanomaterials*, vol. 15, no. 14, pp. 1–15, 2025, doi: 10.3390/nano15141078.
- [11] S. Li, Y. Su, and R. Li, “Splitting of the neutral mechanical plane depends on the length of the multilayer structure of flexible electronics,” *Proc. R. Soc. A*, vol. 472, no. 2190, 2016, doi: 10.1098/rspa.2016.0087.
- [12] B. Yang *et al.*, “Strain effects on halide perovskite solar cells,” *Chem. Soc. Rev.*, pp. 7509–7530, 2022, doi: 10.1039/d2cs00278g.

- [13] L. Sun *et al.*, “A flexible photovoltaic fatigue factor for quantification of mechanical device performance,” *Adv. Funct. Mater.*, vol. 35, no. 19, 2025, doi: 10.1002/adfm.202422706.
- [14] J. Wu *et al.*, “Strain in perovskite solar cells: Origins, impacts and regulation,” *Natl. Sci. Rev.*, vol. 8, no. 8, 2021, doi: 10.1093/nsr/nwab047.
- [15] N. M. Saleh, “Theoretical and practical investigation of the CTPTC performance using fuzzy logic control,” *NTU J. Renew. Energy*, vol. 2, no. 1, pp. 27–33, 2022.
- [16] F. H. Hasan, F. A. Mohammed, A. H. Ahmed, R. A. Hasan, and K. Saleh, “Optimization and simulation of the perturb and observe algorithm for maximum power point tracking in photovoltaic systems,” *NTU J. Renew. Energy*, vol. 9, no. 1, pp. 73–81, 2025.
- [17] F. H. Hasan, S. Algburi, and S. B. Ezzat, “Investigating the impact of internal and external factors on solar cell performance to enhance energy conversion efficiency,” *NTU J. Renew. Energy*, vol. 8, no. 1, pp. 14–23, 2025.
- [18] A. S. T. Hussain *et al.*, “Unlocking solar potential: Advancements in automated solar tracking systems for enhanced energy utilization,” *J. Robot. Control*, vol. 5, no. 4, pp. 1018–1027, 2024.
- [19] R. A. Hasan, M. M. Akawee, and T. Sutikno, “Improved GIS-T model for finding the shortest paths in graphs,” *Babylonian J. Mach. Learn.*, pp. 7–16, 2023.
- [20] R. A. Hasan, T. Sutikno, and M. A. Ismail, “A review on big data sentiment analysis techniques,” *Mesopotamian J. Big Data*, pp. 6–13, 2021.
- [21] S. M. Alqaraghuli and O. Karan, “Using deep learning-based energy-saving framework for software-defined wireless sensor networks,” *Babylonian J. Artif. Intell.*, pp. 34–45, 2024, doi: 10.58496/BJAI/2024/006.
- [22] K. Balasubramani and U. M. Natarajan, “A fuzzy wavelet neural network and hybrid optimization technique for traffic flow prediction,” *Babylonian J. Mach. Learn.*, pp. 121–132, 2024, doi: 10.58496/BJML/2024/012.
- [23] T. Al-Quraishi *et al.*, “Transforming Amazon’s operations: Leveraging Oracle cloud-based ERP with advanced analytics,” *Appl. Data Sci. Anal.*, pp. 108–120, 2024, doi: 10.58496/ADSA/2024/010.
- [24] A. Sengupta and S. Dasgupta, “Real-time cloud-based fish health monitoring using IoT,” *Babylonian J. Internet Things*, pp. 87–93, 2024, doi: 10.58496/BJIoT/2024/011.
- [25] H. J. K. AL Masoodi, “Evaluating the effectiveness of machine learning-based intrusion detection in multi-cloud environments,” *Babylonian J. Internet Things*, pp. 94–105, 2024, doi: 10.58496/BJIoT/2024/012.
- [26] P. R. Kareem, “Performance of PV panel under shaded condition,” *NTU J. Renew. Energy*, vol. 1, no. 1, pp. 22–29, 2020, doi: 10.56286/ntujre.v1i1.25.
- [27] L. Deng, H. Zhao, and X. Wang, “Task offloading and resource allocation for edge-enabled MCC systems,” *Future Gener. Comput. Syst.*, vol. 106, pp. 82–94, 2020.
- [28] A. Saleh *et al.*, “Green building techniques under the umbrella of the climate framework agreement,” *Babylonian J. Mach. Learn.*, pp. 1–14, 2024.
- [29] S. Mahmud, A. Abbasi, R. K. Chakrabortty, and M. J. Ryan, “A self-adaptive hyper-heuristic-based multi-objective optimisation approach for integrated supply chain scheduling problems,” *Knowl.-Based Syst.*, vol. 251, p. 109190, 2022.
- [30] R. A. Hasan, M. M. Akawee, and T. Sutikno, “Improved GIS-T model for finding the shortest paths in graphs,” *Babylonian J. Mach. Learn.*, pp. 7–16, 2023.
- [31] N. M. Saleh, “Theoretical and practical investigation of the CTPTC performance using fuzzy logic control,” *NTU J. Renew. Energy*, vol. 2, no. 1, pp. 27–33, 2022.
- [32] F. H. Hasan, F. A. Mohammed, A. H. Ahmed, R. A. Hasan, and K. Saleh, “Optimization and simulation of the perturb and observe algorithm for maximum power point tracking in photovoltaic systems,” *NTU J. Renew. Energy*, vol. 9, no. 1, pp. 73–81, 2025.